Ecological Modelling 409 (2019) 108736

Contents lists available at ScienceDirect

Ecological Modelling

journal homepage: www.elsevier.com/locate/ecolmodel

Optimizing individual tree detection accuracy and measuring forest uniformity in coconut (*Cocos nucifera* L.) plantations using airborne laser scanning

Midhun Mohan[a,b], Bruno Araujo Furtado de Mendonça[c,*], Carlos Alberto Silva[d,e], Carine Klauberg[f], Acauã Santos de Saboya Ribeiro[g], Emanuel José Gomes de Araújo[c], Marco Antonio Monte[c], Adrián Cardil[h]

[a] Department of Forestry and Environmental Resources, North Carolina State University, 2800 Faucette Drive, Raleigh, NC, 27695, USA
[b] Drone Academy Thailand, Ratchpruek Village Sukkhaprachasun Rd., Bangpood, Prakred, Nonthaburi, 11120, Thailand
[c] Departamento de Silvicultura, Universidade Federal Rural do Rio de Janeiro, Rua da Floresta, Seropédica, RJ, 23897-005, Brazil
[d] Department of Geographical Sciences, University of Maryland, College Park, MD, 20740, USA
[e] NASA Goddard Space Flight Center, 8800 Greenbelt Road, Greenbelt, MD, 20771, USA
[f] Federal University of São João Del Rei – UFSJ, Sete Lagoas, MG, 35701-970, Brazil
[g] Departamento de Engenharia Florestal, Universidade Federal de Viçosa, Viçosa, MG, 36570-000, Brazil
[h] Tecnosylva. Parque Tecnológico de León, 24009, León, Spain

ARTICLE INFO

Keywords:
Lidar point clouds
Canopy density
Forest homogeneity
Uniformity index
Tree window size
Smoothing window size
Adaptive window size
Plantation forestry
Tree count
Irregular tree crown

ABSTRACT

Forest inventory and monitoring is indispensable for coconut (*Cocos nucifera* L.) forest plantation owners as it allows them in assessing tree growth, fruit production rates and vitality of plantations, as well as assists to meet up with the rising market demands by ensuring better yields. Nonetheless, the use of remote sensing techniques for optimizing the management and production of coconut plantations is still at a latent stage. In this paper, we present an airborne laser scanning (lidar) based tree detection method applied for automatically identifying individual coconut trees in a plantation in southeast Brazil. This method locates individual trees by searching treetops on canopy height models (CHM) derived from lidar data through a moving window having fixed treetop window size (TWS). Here, an adaptive TWS approach was implemented as a function of lidar-derived canopy cover (COV, %) along with additional smoothening window sizes (SWS) for enhancing tree detection accuracy. A total of 19 plots characterized by varying levels of canopy cover were used for testing the accuracy of our framework and we were able to obtain an average tree detection accuracy of 86.22%. From a total of 341 trees, 294 trees were detected correctly by the algorithm using adaptive TWS. A low TWS (3x3) value was found to perform best in study plots having COV > 80% and for rest of the cases, a higher TWS (7x7) was perceived suitable. Results were further analyzed and compared, to evaluate the relationship of Individual Tree Detection (ITD) accuracy with varying canopy cover levels, within-plot tree distribution patterns, TWS and SWS values. Proceedings from our work show that appropriate combination of lidar-derived CHMs, local maxima (LM) algorithm and window sizes have the potential to satisfactorily (F-score ˜ 0.90) detect plantation species having irregular canopies such as coconut trees. As an extension of the ITD, estimation of forest uniformity, which gives a measure of the level of homogeneity or heterogeneity of stands, is also performed.

1. Introduction

Forest inventory and monitoring is critical to plantation owners due to its usage in identifying, quantifying and tracking forest cover, growth stages, fruit production rates, wood stocks, optimal harvest times, land characteristics and resource allocation of their plantations (Wulder et al., 2012; Silva et al., 2017a, 2017b; Roise et al., 2016; Schreuder et al., 1993). Over the years, development of remote sensing

* Corresponding author.
E-mail addresses: mmohan2@ncsu.edu (M. Mohan), brunomendonca@ufrrj.br (B.A.F.d. Mendonça), carlos_engflorestal@outlook.com (C.A. Silva), klauberg@ufsj.edu.br (C. Klauberg), acaua.ribeiro@ufv.br (A.S. de Saboya Ribeiro), emanuelaraujo@ufrrj.br (E.J.G.d. Araújo), marcomonte@ufrrj.br (M.A. Monte), adriancardil@gmail.com (A. Cardil).

https://doi.org/10.1016/j.ecolmodel.2019.108736
Received 12 November 2018; Received in revised form 27 June 2019; Accepted 28 June 2019
Available online 25 July 2019
0304-3800/

techniques, computer software and machine learning algorithms, have significantly improved inventory and monitoring methods applied to plantation forestry, and have helped in characterizing forest structure vertically across the landscapes (Ferraz et al., 2015, 2016; Hall et al., 2011; Jaafar et al., 2018). Several recent studies have highlighted the effectiveness of airborne laser scanning (ALS; lidar; Light Detection and Ranging) for individual tree detection (ITD). The prime advantage of utilizing lidar data over aerial imagery for ITD is that being an active sensing technology lidar beams are able to penetrate vegetations and attain more information on the vertical profile of the canopies and individual trees even under poor lighting conditions, whereas aerial imagery cannot (Hodgson and Bresnahan, 2004; Silva et al., 2019).

In fact, research on algorithm creation for ITD dates back to the early 1990s with the local maxima (LM) based algorithm being one of the most prominent methods (Pinz, 1991; Ke and Quackenbush, 2011). LM algorithm assume that high local intensity maxima in the imagery represent treetops (Korpela et al., 2006) and utilizes two major parameters: A Smoothing Window size (SWS) and a Tree Window Size (TWS). Application of smoothing filters help eliminates spurious local maxima caused by spread out tree branches and contorted snags. The TWS parameter allow us to define a fixed boundary within which the algorithm looks for treetops. Although, most of the initial studies on LM, which were based on aerial images, encountered serious flaws resulting in over detection of trees – mostly produced by multiple hits per tree – advancements in lidar technology helped improve this situation as extraction of details on the canopy structure became possible.

As coconut offers versality to its growers, due to its multiple uses – such as food, beverages, cosmetics, and healthcare - the number of foreign investments that support coconut plantations in tropical countries such as Brazil have been on a boom in the past couple of years (Martins and Jesus Junior, 2011; Satyanand, 2009; Bai et al., 2005; Martins and Jesus Junior, 2014). Studies focusing on application of remote sensing techniques for the optimization and management of coconut plantations can possibly assist the coconut plantation sector worldwide in navigating various globally prevailing issues – such as competition from oil palm plantations, improper farming practices, unidentified ecological changes, lack of environmental awareness and several other location-specific issues such as water deficiency and nutrient variations (Saha and Mat, 2018a; Ohler, 1998; Samarajeewa et al., 2001; Choudhury, 2002; Srinivasan, 2002; Saha and Mat, 2018b; Carvalho et al., 2013; de Azevedo et al., 2006; Kahlon et al., 2018). In this regard, ITD of coconut trees can be perceived very helpful as the automatic ITD process helps make the inventory and monitoring processes less time-consuming, more frequent, affordable, and efficient.

In spite of that, detection of individual coconut trees poses great challenges due to the lack of technological awareness among small-scale farmers, irregularly configured coconut canopy structure and limited availability of spatial data with sufficient detail (Edson and Wing, 2011; Andersen, 2009; Saha and Mat, 2018a; Ohler, 1998; Samarajeewa et al., 2001; Choudhury, 2002; Srinivasan, 2002; Saha and Mat, 2018b). Issues faced with ITD of oil palms (a similar tree species, that show resemblance in crown structures and textural features with that of coconut trees) such as overlap of palm crowns of similar heights, incomplete palm crown reconstructions caused due to irregular crown shapes and exposed wind and gust, limitations by class heterogeneity and attendant mixed pixels, and financial constraints for small-scale area can also be viewed as potential hindrances towards optimal ITD of coconut trees (Kattenborn et al., 2014; Nunes et al., 2017; Mayossa et al., 2015; Puttemans et al., 2018; Srestasathiern and Rakwatin, 2014; Teina, 2009; Lelong et al., 2004).

From individually detected trees, tree heights can also be estimated and based on the deviations exhibited by tree heights, forest uniformity indices could be developed for increasing forest productivity (Hentz et al., 2018; Hakamada et al., 2015a; Zucon et al., 2015). In general, if a stand is highly heterogeneous, its final yield can get limited due to the presence of dominant trees, which get greater access to soil nutrients, water, sunlight and fertilizers, reducing availability for the younger and shorter dominated trees (Hakamada et al., 2015a; Luu et al., 2013; Campoe, 2012; Binkley, 2004; Ryan et al., 2010; Boyden et al., 2008; Binkley et al., 2002; Stape et al., 2010; Binkley et al., 2010; Otto et al., 2014). Additionally, by understanding the variation of tree growth rates, we can identify parts of the field affected by soil nutrient deficiency and/or inappropriate level of water availability.

In our research study, we utilize lidar data to detect individual coconut trees at multiple plots of varying canopy cover levels within a coconut plantation located in southeast Brazil. In particular, we are employing a LM based algorithm along with different combinations of TWS and SWS, on lidar-derived CHMs for executing the ITD process; the canopy cover (COV, %) is also computed from lidar, to evaluate its usefulness for optimizing TWS selection. Adding to that, as an extension of ITD, estimation of plot-level uniformity is also performed with an aim to approximate the existing variability in growth rates of trees. For this purpose, PH350 index was computed for each plot.

2. Materials and methods

2.1. Study area

The study area (Fig. 1) encompasses 11 ha of a coconut plantation in a rural settlement located northeast of Japeri municipality, in the state of Rio de Janeiro, Brazil. The elevation of the region ranges from 30 m to 100 m and the climate is characterized as tropical without dry season, defined as Af (tropical rainforest climate) in Koppen classification (Alvares et al., 2013). Annual average precipitation is around 1450 mm; average temperature ranges from a minimum of 20.9 °C in the coolest month (July) to a 26.7 °C in the hottest month (February) (Climate-data.org, 2014). A total of 7 sites, with varying levels of canopy cover, were considered. These sites can be subsumed under three categories – based on experts' opinions after analyzing the aerial imageries of the study area: Type A Stands - plantations with high canopy cover (sites 1, 2 and 3), Type B Stands – plantations with medium canopy cover (sites 4 and 5) and, Type C Stands – plantations with low canopy cover (sites 6 and 7).

2.2. Lidar data collection and processing

The lidar data were acquired through a private company named Topocart and they employed a Leica Geosystems ALS60 sensor scanning with a camera RCD 105 for data acquisition purpose; the survey was conducted on September 2013. Specifications of the lidar system used are summarized in Table 1.

We employed functionalities available in US Forest Service FUSION/LDV3.42 software (McGauchey, 2015) and LAStools (Isenburg, 2015) to perform lidar preprocessing. For ground and non-ground separation, a filtering algorithm based on Kraus and Pfeifer (Kraus and Pfeifer, 1998) was applied. Afterwards, using the classified ground (bare-earth) points, DTM with a spatial resolution of 1.0 m was generated using GridSurfaceCreate function. The GridSurfaceCreate function generates a gridded surface model representing the average elevation for all points within a cell, so that the final surface it produces lies within the bare-earth point set. Subsequently, the heights were normalized using ClipData tool, and it was assured that the z coordinate for each point corresponded to the height above ground and not the orthometric elevation of the single point. The ClipData tool, when used in conjunction with a bare-earth model, allows ground elevations to be subtracted from the return elevations. The Canopy Height Model (CHM) with a spatial resolution of 0.5 m, was built using the pit-free algorithm developed by Khosravipour et al. (2014); the workflow was implemented by following the approach proposed in Isenburg (2015). A pit-free algorithm is a kind of technique that exploits the 3D structure of the tree crowns for removing height variations existing within lidar data; this way, issues associated with data pits – which are irregular

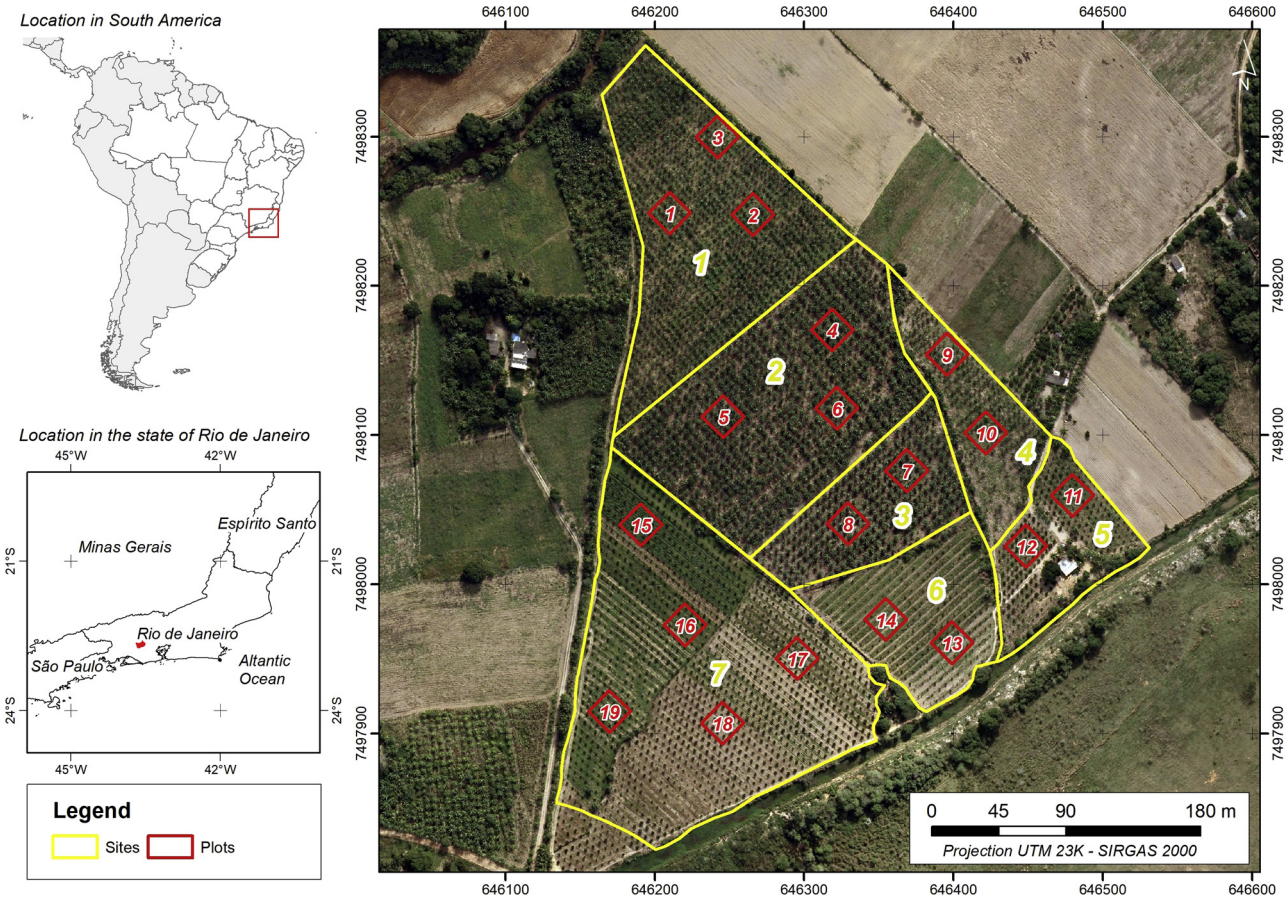

Fig. 1. Location of the study area, plots, and sites of the coconut plantation at northeast of Japeri municipality, in state of Rio de Janeiro (Brazil).

Table 1
Lidar flight parameter characteristics.

Parameters	Values
Flight velocity	120 km/h
Flying height	4,572 m
Laser points m^{-2}	3 points m^{-2}
Pulse Rate	200 kHz
Scan Angle	75°
Scan Pattern	Regular

height variations – present in CHMs can be resolved (Khosravipour et al., 2014, 2013). These pits are usually developed when the first return from lidar is far below the canopy and these impede the accurate extraction of forest parameters from CHMs (Persson et al., 2002; Leckie et al., 2003). Nevertheless, pit-free algorithm incorporates a three-step workflow – that includes i) normalizing the height of the lidar data by replacing the elevation of each point with its vertical height above the ground, ii) constructing one standard CHM using all first returns and multiple partial CHMs based on first returns associated with higher-up vegetation hits and iii) stacking all the previously developed CHMs for creating a final CHM where each cell location has the maximum value across all input rasters – that addresses this issue. Hence, aforementioned approach was selected over alternative choices such as gaussian filtering, which often fails to accurately target the pits and instead alter all pixels of the CHM raster thereby exerting distortion on the tree crown structures (Khosravipour et al., 2013); even then, we tested this surrogate, in the hope of extracting fruitful interpretations.

In parallel, lasclip function from lidR package (Roussel and Auty, 2018) was employed for creating subsets of the lidar points clouds within the study plots. Following this, the point clouds were normalized using lasnormalize function in lidR package (Roussel and Auty, 2018) and COV value for plots were computed from the normalized point clouds using LASmetrics function in rLiDAR package; LASmetrics function allows the user to compute a wide range of LiDAR metrics that statistically describe the lidar dataset (Silva et al., 2017a). All the aforementioned functions were implemented in R software (R Core Team, 2015). COV calculation (see Eq. (1)) was done to test its applicability for improving the selection of TWS parameters in a particular test plot, as listed in previous studies (Silva et al., 2016; Falkowski et al., 2008);this way, an adaptive TWS selection approach was enacted in this study for optimizing ITD accuracy. The height threshold (ht) was set to 0.08 m while calculating COV, so that the potential lidar returns from grass are removed, not at the expense of lidar returns from coconut tree saplings' crowns - whose heights were as low as 0.10 m at some instances.

$$\mathrm{COV}\,(\%) = \left(\frac{\text{Number of lidar first returns above ht}}{\text{Total number of lidar first returns}}\right) * 100 \quad (1)$$

2.3. Individual tree detection and accuracy assessment

For detecting individual coconut trees from CHMs, FindTreesCHM function available in the rLiDAR package in R (Silva et al., 2017a; R Core Team, 2015) was used. The FindTreesCHM function search for treetops in the CHM through a moving window with a fixed TWS (Wulder et al., 2000). As the underlying methodology incorporated for this function is the local maximum algorithm, tree tops found are actually the pixels with maximum heights, within the fixed window (see Fig. 2B); the number of local maxima identified are kept under check by defining a height threshold as well as by applying smoothing filters (Silva et al., 2016; Wulder et al., 2000; Gebreslasie et al., 2011). For our

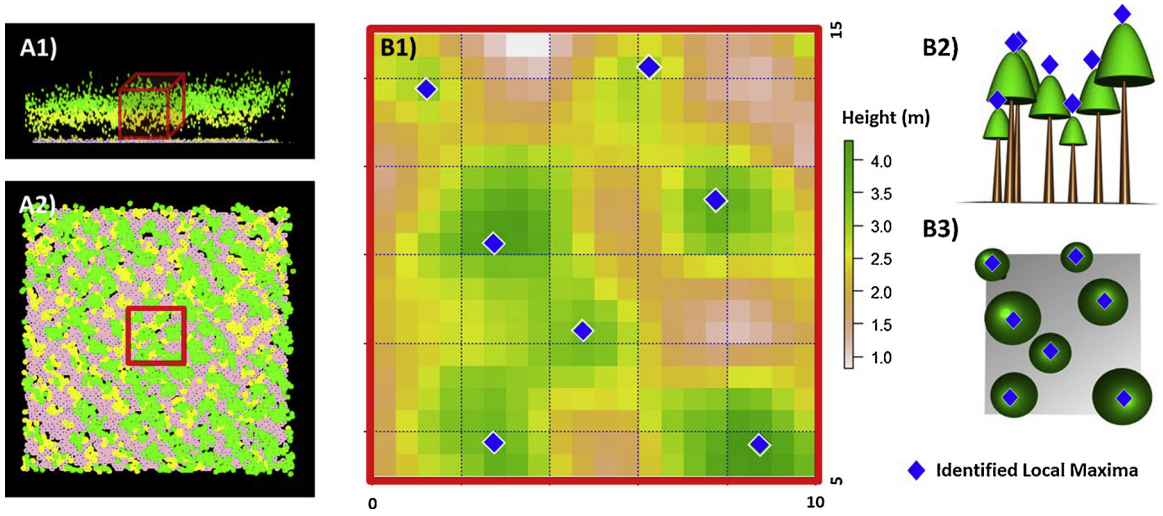

Fig. 2. Exemplification of local maxima (LM) estimation and its alignment with individual tree detection (ITD) process: side view (A1) and top view (A2) of lidar point clouds of a sample study area; LM identification on a subset of the study area (region enclosed by the red square) from the corresponding smoothed canopy height model (B1); side view (B2) and top view (B3) of 3D model of the trees detected by LM algorithm (For interpretation of the references to colour in this figure legend, the reader is referred to the web version of this article.).

study, we selected a total of 19 plots (20 m x 20 m), having an area of approximately 0.04 ha each, randomly from 7 different sites, such that variable canopy cover levels are accounted in the samples. Consequently, we tested the combination of various TWS (3 × 3, 5 × 5, and 7 × 7 pixels) with an unsmoothed CHM as well as with multiple fixed smoothing window sizes (SWS; 3 × 3 and 5 × 5 pixels) and chose parameters accordingly, for attaining an optimal tree detection result; the spatial filter employed was mean filter, as this filter has been found to perform well with trees having irregular canopy structures (Silva et al., 2016). Along with that, the associated tree top heights (*H*) were also noted from the CHMs for further analysis purposes.

For evaluation purposes, initially, the number of trees detected (NTD) per plot using lidar were manually compared with reference data gathered through visual assessment of high resolution imagery – which was created after orthorectifying aerial photos, that were taken along with the LiDAR survey (September 2013) – of the study sites; the spatial resolution of the images were 30 cm and the camera used was a Vexcel Microsoft model UltraCam-X. TWS-SWS combinations that gave best results for each plot were noted and the best-performing TWS-SWS combinations, with respect to COV, were selected for conducting accuracy assessment. A performance assessment in terms of relative error rate (Eq. (2)) was also done, for exploring the individual and combined influence of COV, TWS and SWS in ITD, and the cases for which the relative error was close to 10% were further analyzed. Lastly, accuracy assessment - which involved evaluating in terms of statistical measures such as true positive (TP, correct detection), false negative (FN, omission error), false positive (FP, commission error), recall (r), precision (p) and F-score (F) - was performed on the selected combinations; Eqs. (3)–(5) were adopted from (Li et al., 2012; Goutte and Gaussier, 2005; Sokolova et al., 2006). Here, recall gives us a measure of trees-detected and is inversely related to omission error, precision denotes a measure of correctly detected trees and is inversely related to commission error, and F-score represents the harmonic mean of recall and precision. Fig. 3 illustrates the ITD pipeline implemented in this paper. For validating the ITD-derived tree heights, we measured the tree heights manually from the LiDAR point clouds using FUSION/LDV (see supplementary figure S1) and used them as our reference for comparison.

$$\text{Relative Error (\%)} = \left(\frac{\text{N}^{\text{o}}\text{ tree detected} - \text{N}^{\text{o}}\text{ tree observed}}{\text{N}^{\text{o}}\text{ tree observed}}\right) * 100 \quad (2)$$

$$r = \frac{TP}{(TP + FN)} \quad (3)$$

$$p = \frac{TP}{(TP + FP)} \quad (4)$$

$$F = \frac{2*r*p}{(r + p)} \quad (5)$$

2.4. Plot-level uniformity index estimation

Surprisingly, only a few studies (Hentz et al., 2018; Hakamada et al., 2015a, b; Hakamada, 2012) have explored the possibility of deriving uniformity indices to date, and none focusing on coconut plantations (Luu et al., 2013; Boyden et al., 2008; Stape et al., 2010; Little et al., 2003; Silva, 2005). In these studies, the authors mostly employed the forest uniformity index Pvar50 or PV50 (Hakamada et al., 2015a, b). These entities provide a measure of the accumulated contribution of the smaller trees (50% of the total trees) – in terms of volume in these cases - with respect to the entire stand being considered; the variables being analyzed – such as volume, height, biomass, etc. – can be chosen depending on study purpose. Even though the indices were initially developed based on field data (Schreuder et al., 1993; Gibbs et al., 2007), its variations - such as PH350 - that employ remotely sensed data have also been tested and found applicable for assessing forest uniformity. Former studies (Hentz et al., 2018; Hakamada et al., 2015a, b; Hakamada, 2012) have reported PH350 index to be highly correlated to PV50 and the authors have reported satisfactory results and interpretations from the PH350 index values, especially in case of young plantations (Hentz et al., 2018), where it is not possible to obtain the DBH. Hence, considering the fact that a lot of our stands had coconut saplings, aforementioned index, with variable of importance being tree height, was chosen for this study.

The plot-level uniformity was estimated using the $PH^3 50$ index, which gives a measure of the accumulated contribution of 50% shorter trees – i.e., trees having heights below the 50th percentile tree height - within any given plot (Hentz et al., 2018; Hakamada, 2012). The $PH^3 50$ values (Eq. (6)) were calculated based on the lidar-detected trees, in all the plots, irrespective of whether the algorithm exhibited discrepancies – such as detection of nonexistent trees (commission errors), or failure in detecting actually existing trees (omission errors). This strategy was incorporated as in real-time applications we will not be able to detect if these errors are occurring or not. The equation for $PH^3 50$ index is as follows:

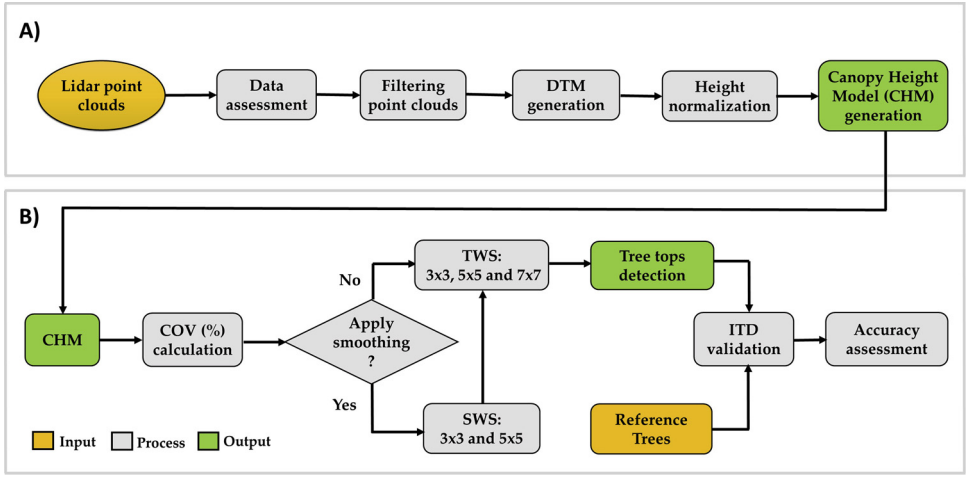

Fig. 3. Workflow of A) lidar data pre-processing and B) local maxima based Individual Tree Detection methodology.

$$PH^3 50 = \frac{\sum_{i=1}^{n/2} H_i^3}{\sum_{i=1}^{n} H_i^3} \quad (6)$$

Where, H_i^3 denotes the cubic power of the ith tree height and n is the sorted – i.e., trees are initially sorted from smallest to the largest with respect to tree heights - tree number. Adhering to the observations made by Hakamada et al. (2015a), we considered the plots having PH350 index within the range of 0.37 and 0.50 to be homogeneous plots. Fig. 4 provides a pictorial representation of the step-by-step processes involved in $PH^3 50$ index estimation. The first step (Fig. 4A1), being the tree top identification – with the algorithm detecting 18 trees in this case - allows us to extract individual tree heights, and we estimate the 50th tree height percentile (Fig. 4A2) from the obtained values. Afterwards, for calculating $PH^3 50$ index, we determine the ratio of sum of cubes of tree heights of trees below 50th tree height percentile and sum of cubes of tree heights of all the trees in a given plot (see Eq. (6)). In part B1 of the Fig. 4, the x-axis denotes the trees, which are ranked - from the shortest to the tallest (i.e., tree 1 has the lowest height value and the height keeps increasing till tree 18, which is the tallest tree). On the y-axis, corresponding $PH^3 50$ values are provided. The green line presents the case of a hypothetical homogenous plot, having maximum uniformity; this can be perceived as an equality line. In this case, 50% of (shorter) trees would account for 50% of total $PH^3 50$; which means, $PH^3 50$ index will be 0.5. The orange line represents the sample under consideration (figure 4A1) and in this case 50% of the shorter trees correspond to only 34% of total $PH^3 50$ resulting in a $PH^3 50$ index of 0.34 – indicating the mildly heterogenous nature of the plot.

3. Results

With varying combinations of TWS and SWS, we observed differences in accuracy rates for ITD (see Table 2). The best combination for ITD was found to be for 7 × 7-5 × 5 TWS-SWS combination. In this case, 7 out of the total 19 instances gave "best" tree detection results; here "best" implies closeness of number of trees detected (NTD) to the reference tree count (N). Also, it was noted that 1 plot of Type A plantations, 3 plots of Type B Stands and 5 plots of Type C Stands had their N and NTD values identical. In some cases (see Table 2; plot IDs: 4, 5, 10, 12, 15 and 19), multiple combinations of TWS and SWS were found to provide similar results.

In general, an increase in COV was found to be detrimental towards the tree detection ability of the algorithm; for very high canopy cover plots (i.e., COV > 80%) TWS-SWS combination of 3 × 3–5 × 5 gave best results in 3 out of 4 cases. Nevertheless, the impact of varying TWS and SWS was not having a linear relationship with the tree detection accuracy. The total number of detected trees in 3 × 3 TWS revealed better results with increasing SWS values. Whereas, for 5 × 5 TWS and 7 × 7 TWS, both 3 × 3 SWS and 5 × 5 SWS were found to perform equally well. This non-uniform trend in ITD encouraged us to further analyze the possibilities of relationships existing between TWS and SWS, as well as with canopy cover levels. Without the smoothing filter (NF), ITD showed near-zero accuracy in all the cases.

By calculating relative error for all the cases (Table 3), we were able

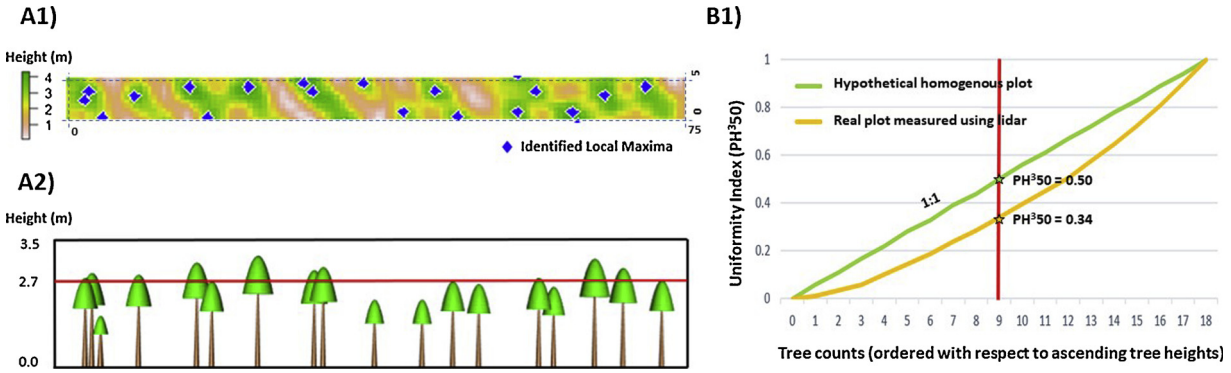

Fig. 4. Steps involved in the estimation of uniformity index $PH^3 50$: tree tops detected from canopy height model of a sample plot (A1); identification of the 50th tree height percentile (represented by the red horizontal line; A2) and calculation of sum of H^3 for all the trees as well as for the trees below 50th percentile for estimating $PH^3 50$ index; graphical representation of $PH^3 50$ calculation (B1) and comparison of the lidar-derived uniformity index of a sample plot with the uniformity index of a hypothetical homogenous plot (For interpretation of the references to colour in this figure legend, the reader is referred to the web version of this article.).

Table 2
Number of trees detected (NTD) in each plot for varying tree top window size (TWS) and smoothing window size (SWS). Also shown are % canopy cover (COV) and the true number of trees per plot (N). Values in bold represent best results for each plot.

Sites	Plot (ID)	COV	Ref. (N)	TWS								
				3 × 3			5 × 5			7 × 7		
				SWS			SWS			SWS		
				NF	3 × 3	5 × 5	NF	3 × 3	5 × 5	NF	3 × 3	5 × 5
1	1	81.53	24	358	40	29	158	**25**	20	96	19	16
	2	82.57	26	365	32	**23**	157	19	19	108	14	12
	3	80.12	21	311	27	**21**	133	20	16	85	14	16
	4	80.02	19	368	39	**21**	159	25	15	96	**17**	12
2	5	72.95	14	408	32	25	159	21	**17**	99	19	**11**
	6	73.37	16	379	40	26	182	20	13	114	**18**	**13**
3	7	71.96	14	393	42	22	160	21	16	100	17	**15**
	8	79.66	16	383	40	21	194	24	13	117	**18**	13
4	9	68.95	20	345	31	21	159	**20**	17	111	18	16
	10	65.48	16	397	30	23	166	19	**17**	106	13	**15**
5	11	63.96	24	314	**24**	20	160	21	19	145	20	19
	12	66.36	19	275	22	20	137	**19**	**19**	109	**19**	18
6	13	51.31	15	356	27	18	137	**15**	14	99	14	14
	14	39.73	12	397	37	29	201	29	17	134	17	**13**
7	15	42.60	18	342	32	**15**	148	**15**	**15**	95	14	13
	16	57.76	17	315	28	16	133	18	16	100	**17**	16
	17	54.85	16	334	26	18	147	19	17	100	17	**16**
	18	61.58	18	294	**18**	16	110	16	16	97	16	16
	19	56.26	16	339	22	**16**	135	**16**	**16**	108	**16**	**16**
Total			341	6673	589	399	2935	383	312	2019	317	280

to choose satisfactory (error % close to ± 10) observations and analyze the individual as well as combined influence of canopy cover levels, TWS and SWS towards tree detection accuracy. In 13 cases – 3 plots of Type A Stands, 4 plots of Type B Stands and 6 plots of Type C Stands – ITD algorithm of varying TWS and SWS combinations were able to detect trees with satisfactory accuracy. On a combined basis, 7 × 7 TWS and 5 × 5 SWS gave the best results in maximum number of instances (8 cases). However, for cases where COV was greater than 80%, 3 × 3–5 × 5 TWS-SWS combination gave better (less than or close to ± 10%) relative error values. Therefore, while performing accuracy assessment (Table 4), in plots where COV was greater than 80%, 3 × 3–5 × 5 TWS-SWS combination was selected and for rest of the cases, 7 × 7-5 × 5 TWS-SWS was considered; we obtained recall (r), precision (p) and F-Score values of 0.87 (range: 0.72 to 1.00), 0.94 (range: 0.69 to 1.00) and 0.90 (range: 0.75 to 1.00) respectively. A count of 294 (86.22%) successful tree tops was reported from the ITD process. From a total of 341 trees, the algorithm missed 47 trees and falsely detected 24 trees, giving an estimate of 318 trees. It also became

Table 3
Test results on relative error rate tolerance, determined by comparing the number of trees detected (NTD) to the observed tree inventory number (N). Values in bold represent the best results (relative error is below 10%).

Sites	Plot (ID)	COV	Ref. (N)	TWS								
				3 × 3			5 × 5			7 × 7		
				SWS			SWS			SWS		
				NF	3 × 3	5 × 5	NF	3 × 3	5 × 5	NF	3 × 3	5 × 5
1	1	81.53	24	1391.7	66.7	20.8	558.3	**4.2**	−16.7	300.0	−20.8	−33.3
	2	82.57	26	1303.8	23.1	−11.5	503.8	−26.9	−26.9	315.4	−46.2	−53.8
	3	80.12	21	1381.0	28.6	**0.0**	533.3	**−4.8**	−23.8	304.8	−33.3	−23.8
2	4	80.02	19	1836.8	105.3	10.5	736.8	31.6	−21.1	405.3	−10.5	−36.8
	5	72.95	14	2814.3	128.6	78.6	1035.7	50.0	21.4	607.1	35.7	−21.4
	6	73.37	16	2268.8	150.0	62.5	1037.5	25.0	−18.8	612.5	12.5	−18.8
3	7	71.96	14	2707.1	200.0	57.1	1042.9	50.0	14.3	614.3	21.4	**7.1**
	8	79.66	16	2293.8	150.0	31.3	1112.5	50.0	−18.8	631.3	12.5	−18.8
4	9	68.95	20	1625.0	55.0	**5.0**	695.0	**0.0**	−15.0	455.0	−10.0	−20.0
	10	65.48	16	2381.3	87.5	43.8	937.5	18.8	**−6.3**	562.5	−18.8	**−6.3**
5	11	63.96	24	1208.3	**0.0**	−16.7	566.7	−12.5	−20.8	504.2	−16.7	−20.8
	12	66.36	19	1347.4	15.8	**5.26**	621.1	**0.0**	**0.0**	473.7	**0.0**	**−5.3**
6	13	51.31	15	2273.3	80.0	20.0	813.3	**0.0**	**−6.7**	560.0	**−6.7**	**−6.7**
	14	39.73	12	3208.3	208.3	141.7	1575.0	141.7	41.7	1016.7	41.7	**8.3**
7	15	42.60	18	1800.0	77.8	−16.7	722.2	−16.7	−16.7	427.8	−22.2	−27.8
	16	57.76	17	1752.9	64.7	**−5.9**	682.4	**−5.9**	**−5.9**	488.2	**0.0**	**−5.9**
	17	54.85	16	1987.5	62.5	12.5	818.8	18.8	**6.3**	525.0	**6.3**	**0.0**
	18	61.58	18	1533.3	**0.0**	−11.1	511.1	−11.1	−11.1	438.9	−11.1	−11.1
	19	56.26	16	2018.8	37.5	**0.0**	743.8	**0.0**	**0.0**	575.0	**0.0**	**0.0**
Total			341	1856.9	72.7	17.0	760.7	12.3	−8.5	492.1	−7.0	−17.9

Table 4
Accuracy assessment results for the best TWS-SWS combinations – 3 × 3–5 × 5 (COV > 80%) and 7 × 7–5 × 5 (COV ≤ 80%): False Positive (FP), False Negative (FN), True Positive (TP), recall (r), precision (p) and F-score (F) statistics parameters. Here, Ref. (N) is the reference number of trees per test plot and Lidar denotes the number of trees detected using lidar.

Sites	Plot (ID)	COV (%)	Number of Trees detected							
			Ref. (N)	Lidar	FP	FN	TP	r	p	F
1	1	81.53	24	29	9	4	20	0.83	0.69	0.75
	2	82.57	26	23	3	6	20	0.77	0.87	0.82
	3	80.12	21	21	2	2	19	0.90	0.90	0.90
2	4	80.02	19	21	6	4	15	0.79	0.71	0.75
	5	72.95	14	11	0	3	11	0.79	1.00	0.88
	6	73.37	16	13	1	4	12	0.75	0.92	0.83
3	7	71.96	14	15	1	0	14	1.00	0.93	0.97
	8	79.66	16	13	0	3	13	0.81	1.00	0.90
4	9	68.95	20	16	0	4	16	0.80	1.00	0.89
	10	65.48	16	15	1	2	14	0.88	0.93	0.90
5	11	63.96	24	19	0	5	19	0.79	1.00	0.88
	12	66.36	19	18	0	1	18	0.95	1.00	0.97
6	13	51.31	15	14	0	1	14	0.93	1.00	0.97
	14	39.73	12	13	1	0	12	1.00	0.92	0.96
7	15	42.60	18	13	0	5	13	0.72	1.00	0.84
	16	57.76	17	16	0	1	16	0.94	1.00	0.97
	17	54.85	16	16	0	0	16	1.00	1.00	1.00
	18	61.58	18	16	0	2	16	0.89	1.00	0.94
	19	56.26	16	16	0	0	16	1.00	1.00	1.00
Total			341	318	24	47	294	0.87	0.94	0.90

Table 5
Accuracy assessment results for the best TWS-SWS combinations with respect to lidar-derived COV (%) ranges: False Positive (FP), False Negative (FN), True Positive (TP), recall (r), precision (p) and F-score (F) statistics parameters. Here, Ref. (N) is the reference number of trees per test plot and Lidar denotes the number of trees detected using lidar.

COV (%)	Number of Trees detected							
	Ref. (N)	Lidar	FP	FN	TP	r	p	F
> 80	90	94	20 (22.22%)	16 (17.78%)	74 (82.22%)	0.82	0.79	0.80
≤ 80	251	224	4 (1.59%)	31 (12.35%)	220 (87.64%)	0.88	0.98	0.93
Overall	341	318	24 (7.04%)	47 (13.78%)	294 (86.22%)	0.87	0.94	0.90

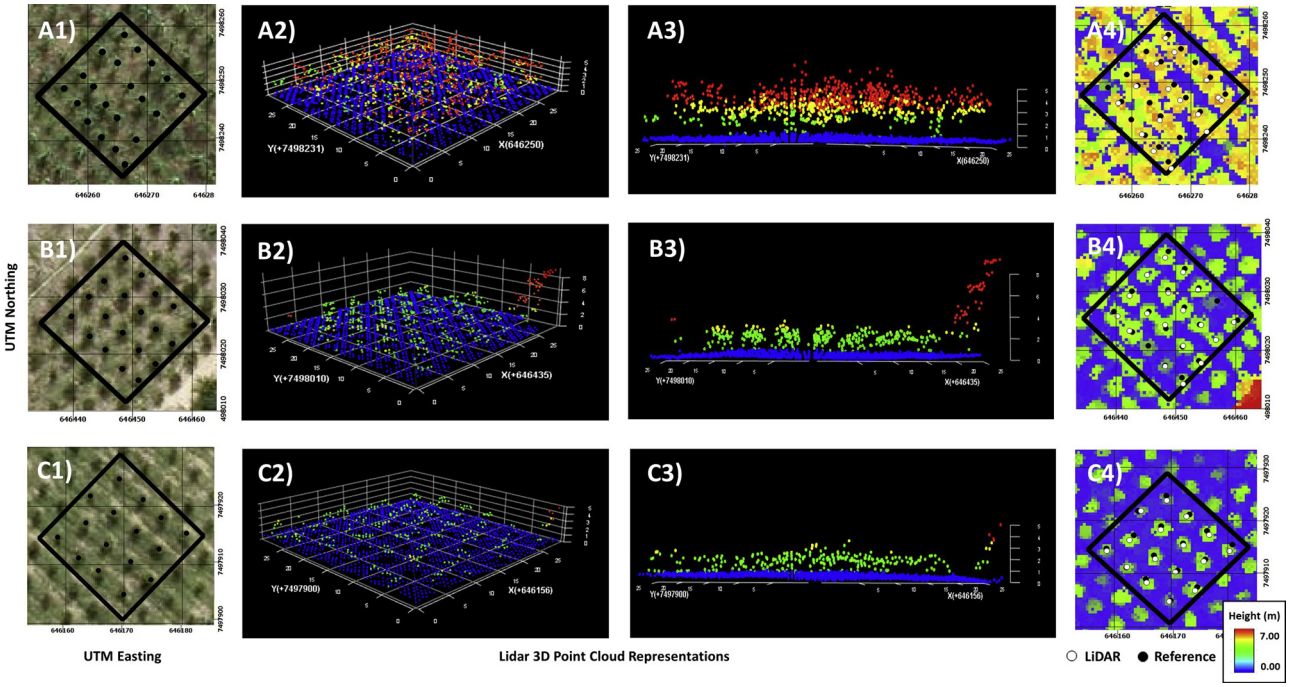

Fig. 5. Field tree reference locations, 3D point cloud visualization, side view of lidar point clouds, and ITD results for a sample Type A Stand (A1-A4), a Type B Stand (B1-B4) and a Type C Stand (C1-C4) respectively.

Table 6
Summary statistics of lidar-derived tree heights and $PH^3 50$ values at plot-level; here, SD denotes Standard Deviation.

Sites	Plot (ID)	Lidar-derived Tree Heights				$PH^3 50$
		Min	Max	Mean	SD	
1	1	2.10	4.33	3.55	0.57	0.3310
	2	1.88	4.29	3.84	0.49	0.4263
	3	0.57	4.53	2.61	1.01	0.1484
2	4	4.74	5.93	5.30	0.31	0.4062
	5	4.56	14.79	5.93	2.97	0.1432
	6	4.20	6.69	5.35	0.70	0.3136
3	7	3.50	5.18	4.37	0.43	0.3953
	8	1.39	4.86	3.40	0.86	0.3092
4	9	4.28	5.65	4.95	0.37	0.4571
	10	4.20	6.01	5.09	0.51	0.3504
5	11	0.41	1.78	1.02	0.39	0.1550
	12	0.76	2.16	1.74	0.33	0.3291
6	13	0.46	1.22	0.81	0.22	0.1994
	14	0.09	0.79	0.30	0.19	0.0432
7	15	0.65	1.49	1.11	0.26	0.2104
	16	0.87	1.95	1.41	0.32	0.2521
	17	0.56	1.62	1.13	0.28	0.2549
	18	1.16	1.89	1.55	0.19	0.3599
	19	0.56	1.70	1.20	0.37	0.2134

evident that, in plots with COV lesser than 80%, average tree detection accuracy (87.64%) and omission error (12.35%) were comparatively better than for the cases where COV was greater than 80% (average ITD accuracy was 82.22% and omission error was 17.78%; see Table 5). Adding to that, with respect to F-score and commission error values, study plots with COV less than 80% showed significantly stronger results (F-score was 0.93 and commission error was 1.59%) compared to plots where COV was greater than 80% (F-score was 0.80 and commission error was 22.22%). Illustrations of 3D lidar point clouds of plots with varying canopy cover levels and their corresponding ITD results, with respect to the reference trees, are presented in Fig. 5.

On evaluating the range of tree heights obtained from lidar, we noticed the standard deviations to vary between 0.19 and 2.97. Even though the average tree heights were below 6 m in all the cases, for plot 5, we obtained a maximum tree height of 14.79 m. Using these derived heights, $PH^3 50$ indices were calculated and they ranged from 0.0432 to 0.4571. Out of the 19 plots, only 4 were found to exhibit high levels of homogeneity. Summary statistics of plot-level lidar-derived tree heights and associated $PH^3 50$ values are presented in Table 6. We also estimated the coefficient of determination (R^2) for ITD-derived tree heights and reference tree heights and obtained an R^2 value of 0.98 (see supplementary figure S2).

4. Discussion

In the past few decades, lidar data has found a stronghold in the realm of ITD based forest inventory applications - due to its ability in estimating tree level attributes such as crown size, DBH, crown close and canopy structure from delineated trees with satisfactory accuracies (Silva et al., 2017a; Zhen et al., 2016; Zhang et al., 2010; Bai et al., 2005; Harding et al., 2001; Duncanson and Dubayah, 2018). Additionally, ongoing advancements in optical remote sensing, hyperspectral imagery, UAV applications and their combinations are also paving ways to enhance ITD initiatives within the forestry sector

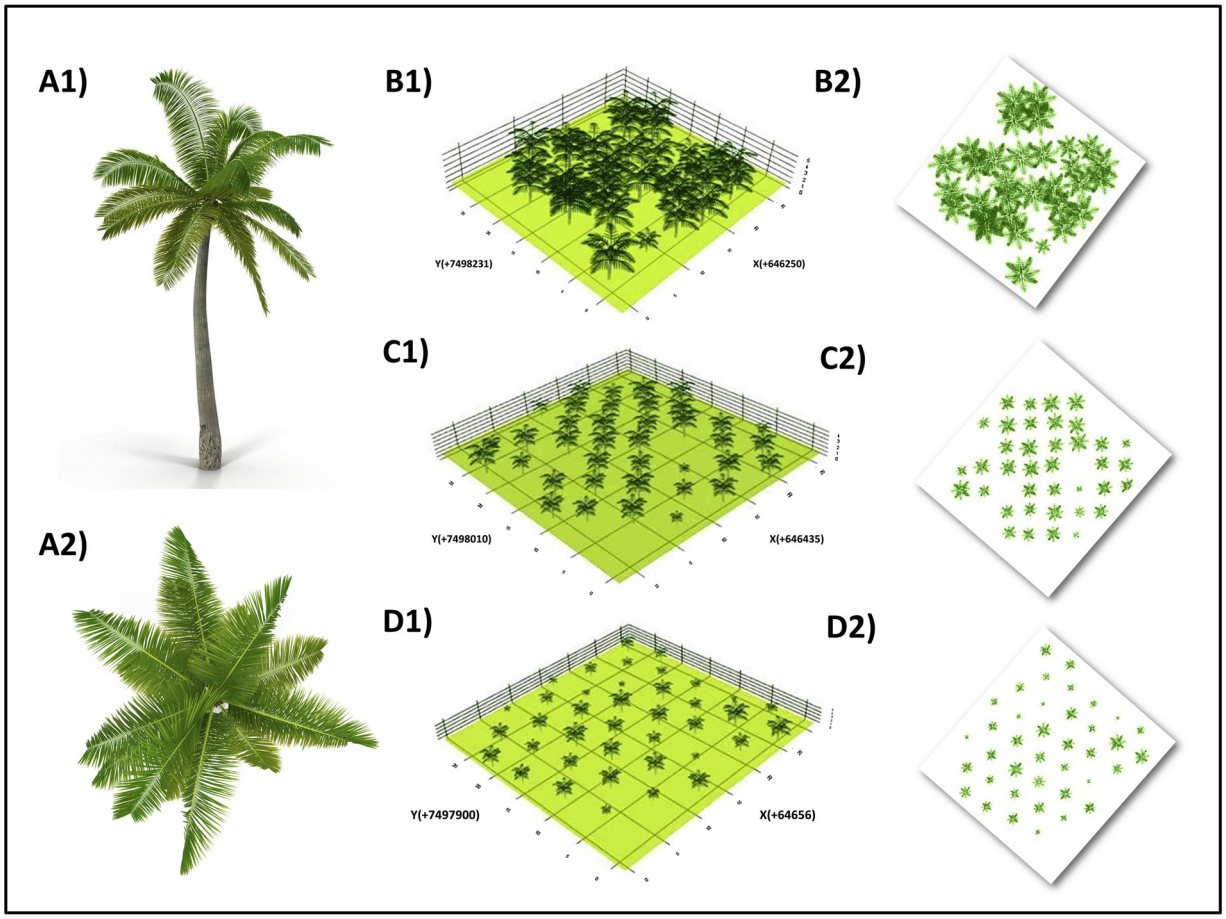

Fig. 6. Illustration of canopy cover levels: side view (A1) and top view (A2) of a 3D coconut tree model; 3D view (B1-D1) and top view (B2-D2) of canopies of a sample Type A Stand, Type B Stand and Type C Stand respectively.

(Mohan et al., 2017; Xiao et al., 2018; Dempewolf et al., 2017; Cardil et al., 2017, 2019). While remote sensing techniques, especially lidar, has become a promising source for performing ITD, its applications have been limited to tropical forests, mixed conifer forests, eucalyptus plantations and pine plantations in several countries, primarily due to data constraints and challenging canopy structures that variant species possess (Ferraz et al., 2016; Ke and Quackenbush, 2011; Féret and Asner, 2013; Pont et al., 2015; Jeronimo et al., 2018). Hence supplemental studies are required, tested with wide variety of cultures and vegetation covers, to confirm the proposed advantages of using airborne laser scanning for ITD.

In our study, we evaluated the applicability of a LM based algorithm for detecting and delineating individual coconut trees, which are rarely studied from a remote sensing perspective, in a plantation comprising of sites with variable canopy cover levels; the basic assumptions of the algorithm being that, each imaged tree crown has a single 'brightest spot' with darker areas between tree crowns (Larsen et al., 2011; Gougeon and Moore, 1988). In accordance with the underlying assumption, we observed the tree tops being represented as 'brightest spots' within the CHMs and depending on the varying levels of canopy covers – from high to low – there occurred an evident increase in darker areas between the 'brightest spots' (blue colored region in Fig. 5(A4-C4)). Coconut tree crowns, because of its irregular canopy cover and often slanted stems, were expected to be comparatively harder to detect and isolate (Fig. 6A). Notwithstanding the potential limitations, selection of a LM approach and testing of different combinations of SWS and TWS proved beneficial for achieving optimal accuracy with the tree top detections. Employing COV variable – with a threshold of 80%, which was relatively higher than the thresholds applied in previous studies (Silva et al., 2016; Falkowski et al., 2008) - as a criterion for adapting the TWS also enabled us to substantially improve the average tree detection accuracy from 79.77% - when only the best TWS-SWS combination (7 × 7-5 × 5) was applied for all the plots (see supplementary table S1) – to 86.22%. This in turn underscores the ability of our proposed methodology for isolating individual trees having irregular tree crowns even in dense canopy plantations. Also, as noted in previous studies (Silva et al., 2016; Khosravipour et al., 2014) a choice of mean filter smoothing with pit-free CHMs gave superior results compared to other commonly employed filter techniques; Gaussian-based approaches were tested as alternatives, however, since coconut tree crowns are acutely asymmetrical, unlike conifers which tend to have a more regular (conical) shape, the results were not at par to the findings obtained using the formerly mentioned method.

The accuracy rates for ITD - which were verified in terms of precision, recall and F-score - shows that successful combinations of TWS and SWS can achieve satisfactory detection results for coconut plantations. Based on the results from the relative error % table (Table 4), we deduced that with the increase in canopy cover, accurate ITD becomes more challenging in case of coconut plantations. This can be attributed to issues associated with occlusion, shadows, variation in light reflectance, canopy overlap and closure, size, and tree spacing as listed in similar studies (Hyyppä et al., 2008; Silva et al., 2016; Zhen et al., 2016; Wulder et al., 2003; Asner and Heidebrecht, 2002). Even though, from Table 4 (ITD) it was found that for plots with COV greater than 80%, a TWS-SWS combination of 3 × 3–5 × 5 provided the best result, in Table 5 (relative error % estimation), we noticed that 5 × 5 − 3 × 3 combination gave satisfactory results in two instances as opposed to 3 × 3–5 × 5 combination which met the cut-off in only one case. However, the relative % error for plots 2 and 4 were very close to 10%–11.5 % and 10.5% respectively – which corroborates the previously observed pattern.

In general, for plots in Type A (high canopy cover) Stands, TWS of 3 × 3 and SWS of 5 × 5 gave the best results. Inaccurate estimation of results happened in alternative TWS-SWS combinations can be related with the irregular canopy of the coconut trees, which has many leaves identified with the local maximum. This can be a serious hurdle in plots having high canopy covers, especially when there occur several matured trees (Fig. 6B).

For plots in Type B (medium canopy cover) stands, effects of TWS-SWS on tree detection enhancement was limited; all the TWS-SWS combinations, expect for NF, were able to identify tree tops of at least one plot with satisfiable accuracy. In alignment to the observations made by previous studies densities (Hyyppä et al., 2008; Silva et al., 2016), we noticed that a lower TWS of 3 × 3 was more effective in ITD when tree counts were high (N = 24). Taking into consideration the high performance exhibited by lower TWS in ITD, for cases where tree count was relatively high (N ≥ 20), it can be inferred that number of trees detected is inversely proportional to the TWS. Adding to that, precision was also found to reduce with decreasing TWS. In our case, the plots with COV > 80%, where 3 × 3 TWS was applied, showed high commission error rate - which implies low precision. Furthermore, in most cases, at plots where the tree heights are relatively higher, chances of obstructions to lidar pulses will be lower, and this helps in generating more accurate CHM models and thereby better ITD accuracy. This might have partially contributed to the aberrations in findings revolving plot 8, which has a COV close to 80%. Here, around half of the total trees were saplings and the remaining half comprised of taller trees with larger crown size areas. Nonetheless, this inference was not able to be made by interpreting uniformity index values. The sizable change in height differences would have enabled a higher TWS to make better tree count approximation as compared to lower TWS; also, the tree count was low in plot 8, compared to other plots having COV > 80%. TWS of 5 × 5 and 7 × 7 performed in an identical manner when tree count was below 20.

Moreover, we were curious to explore the reasons why, among the 4 plots of Type B Stands, only the trees in plot 10 were not able to be detected with 100% accuracy by any TWS-SWS combination. We expect this anomaly to be arising from the differences in within-plot tree distribution and canopy gap patterns (see Fig. 7). This further implies that multiple plots having similar canopy cover values might behave differently to ITD algorithm depending on how the overall arrangement of trees are within each plot; and also, at times, perhaps, contingent on within-plot tree height distributions as well, as presumed in the case of plot 8. Based on the algorithm assumptions, a uniform distribution like that of study plot 12 (Fig. 7C) would be easier to detect for the algorithm than an indented distribution exhibited in plot 10 (Fig. 7D) where tree crowns have a higher level of overlaps along with uneven canopy gaps. Nevertheless, since we had only taken 4 plots into consideration, extensive research for understanding the influence of canopy gap patterns and within-plot tree distribution for ITD is highly recommended before drawing conclusions (Schneider and Larson, 2017; Nyamgeroh et al., 2018; White et al., 2018; Bagaram et al., 2018).

Plots in Type C (low canopy cover) Stands gave satisfactory results for 6 in 7 plots (19 out of 63 TWS-SWS combination cases) with multiple combinations of TWS and SWS yielding optimal predictions; also, an average precision value of 0.99 and an average F-score of 0.95 was attained in this case. Therefore, it can be inferred that when the trees are widely spaced - as in study plot 19 (figure 6D) - the algorithm's efficiency in detecting trees correctly is very high; here, combinations of TWS and SWS have comparatively minor influence on ITD performance. Identical to the findings in Type A and Type B Stands, NF cases did not yield any compelling results in Type C Stands either; this was because of the fact that the irregular tree crowns of the coconut trees cause multiple local maxima to be detected on a single tree crown, unless smoothed, thereby resulting in extreme overestimation of tree counts.

Considering the overall tree detection results, we noticed that there occurred no specific linear tree detection trends with respect to the TWS-SWS combinations, which can be attributed to the complexity arising from various levels of canopy covers and/or biological features associated with the coconut canopy crown structures. Notwithstanding this lack of explicit relationships, based on our findings, using a 7 × 7-

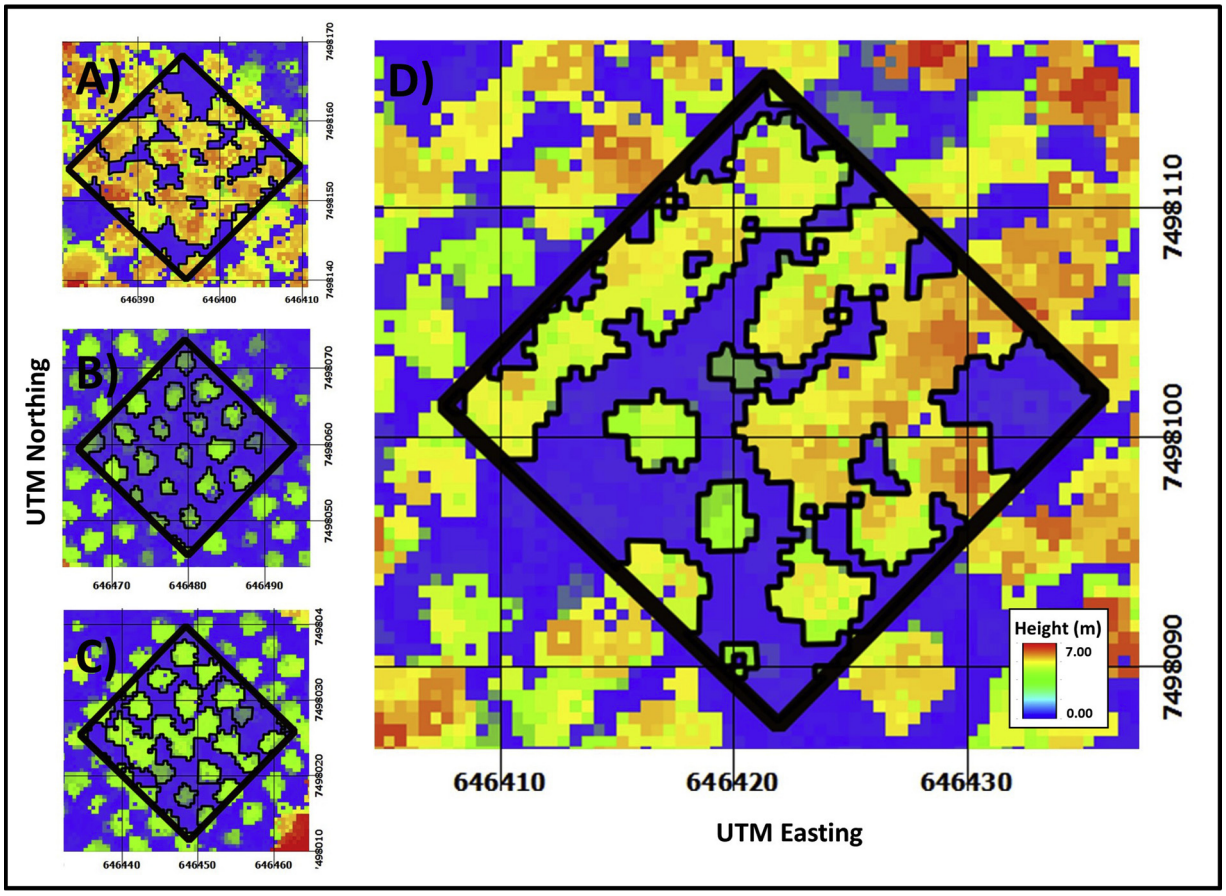

Fig. 7. Within-plot tree distributions and canopy gap patterns (**outlined in black**) of Type B Stands: A) Plot 9, B) Plot 11, C) Plot 12 and D) Plot 10.

5 × 5 or 3 × 3–5 × 5 TWS-SWS combination can be viewed as reliable strategies. Nonetheless, while employing lower (3 × 3) TWS, the commission error rate is expected to very high, due to the over-estimation of tree crowns it makes. On the other hand, the former combination which adopted a higher (7 × 7) TWS had a commission error of only 2.34%. Nevertheless, the 7 × 7 TWS and 5 × 5 SWS combination suffered from underestimation of trees, majorly in plantations with high canopy cover - out of the 69 missed trees, 48 trees were missed while performing ITD in Type A Stands (see supplementary table S1). Hence, this combination is not recommended for plantations similar to the Type A Stands described in this study; for performing ITD in coconut plantations, selecting suitable TWS based on COV, similar to what we did here, is advised. Also, from Table 3, we noted that 5 × 5-3 × 3 TWS-SWS combination performed well in comparison with the previously mentioned combinations. However, since, our final objective was more inclined to pinpointing maximum number of trees extracted that are relevant (i.e., high precision), rather than on the number of relevant trees that are extracted, this combination which had high commission error possibility (Table 3) was not further evaluated. At times, for larger areas, taking a consistent TWS and SWS combination might seem appropriate and time efficient. However, in this case, performance variations can happen if multiple canopy cover levels, tree distribution patterns and/or forest types are present, as observed in our situation as well as in previous studies (Lindberg and Hollaus, 2012; Asner and Heidebrecht, 2002; Kwak et al., 2007).

From the obtained relative error % values (Table 3) for ITD with 7 × 7-5 × 5 TWS-SWS combination (Table 3), it can be noted that even when we increase the relative error % allowable from 0% to 10%, the number of satisfactory results in case of Type A Stands is minimal. Also, there occurred two cases – plot 2 (-11.5%) and plot 4 (10.5%) – where the values were very close to the cut-off limit, which tacitly states that unconditionally relying on relative error % for evaluating ITD efficiency of TWS-SWS combinations can be both erroneous and misleading. On the contrary, for Type B and Type C Stands, additional TWS-SWS combinations acquired satisfactory accuracy with increasing the relative error %, denoting an ease in selecting TWS-SWS combinations. Among the plots in Type C Stands, only for plot 15 we did not find any suitable TWS-SWS combination. Here, two pertinent concerns were accounted. Firstly, for few trees on edges, a major part of their crowns was found to be slanted and leaning outside of the plot perimeter; at times application of a buffer on the study plots, might help address issues associated with slanted tree crowns (Monnet et al., 2010). Secondly, even though all the trees in Type C Stands had adequate amount of spacing between them, some trees had their pinnate leaves spread out, making it hard to be identified from the CHMs. These issues might have caused most of the TWS-SWS combinations to inaccurately estimate the number of tree tops.

Similarly, for plot 14, of the Type C Stands, the algorithm was not able to detect trees with 100% efficiency using any of the TWS-SWS combinations, even though the tree count was only 12. Nevertheless, 100% recall was achieved when 7 × 7-5 × 5 TWS-SWS combination was applied. Meanwhile, plot 19 was found to provide the maximum number of satisfactory results; here, 5 different TWS-SWS combinations were able to obtain 100% accuracy in tree detection. This was a Type C plot with minimum level of canopy cover and very low number of trees which were regularly spaced. Also, three other plots in Type C Stands (plots 13, 16 and 17) and one plot in Type B Stands (plot 12) provided above average results (i.e., at least 3 different TWS-SWS combinations resulted in high accuracy results). Plots of Type C Stands and Type B Stands (except plot 11), where the NTD and N values were found equal (i.e., relative error % = 0), generally comprised of coconut trees with low canopy crown area and closely packed pinnate leave structures; the

wide and organized spacing in-between individual tree crowns would have enabled ITD algorithm to have 100% accuracy in these cases. For the plot 3, belonging to Type A Stands, where relative error % was found to be 0, tree spacing was well structured and canopy gap irregularities were minimal. This might have permitted a lower value TWS in effective tree detection (Silva et al., 2016). Nevertheless, further analysis involving accuracy assessment in terms of precision, recall and F-score is required for confirming our inferences on the ITD trend observed in the aforementioned study plots.

Average tree density is another principal factor that has been found to be influential towards TWS-SWS selection and ITD in plantations species. Previously conducted studies recommend adopting a small SWS for efficient ITD in areas having high plantation densities (Hyyppä et al., 2008; Silva et al., 2016). This is because, as observed from our results, a lower SWS results in estimating larger number of tree tops and thereby achieves better prediction accuracy when dealing with dense forest plots having a colossal amount of tree. Nevertheless, this pattern was not highly perceivable (except for the plot 3) in our study as all our study plots were parts of a plantation - which was developed in a way to have equal number of coconut trees separated by uniform spacing throughout; the irregular shape of coconut tree crowns might have also contributed to this anomaly. As previously stated, the differences in average tree density between plots were expected to be nominal in our case. Even then, we did notice minor changes in the number of trees being reported from the survey, which we expect to result from issues related to seedling mortality rates, natural hazards, and/or rapid weather changes. Additionally, preceding studies have also mentioned about the advantages of using a high TWS for low canopy cover areas (Hyyppä et al., 2008; Silva et al., 2016). However, we did not notice such a trend either; probably because of the equally spaced trees, which made the detection of tree tops a less complicated process. Despite that, in consistent with recent studies, we observed that ITD algorithm, in overall, performed better in cases with open canopies compared to areas with dense canopy covers (Koukoulas and Blackburn, 2005; Pinz, 1991). Therefore, we expect the proposed ITD parameter combinations to work best for regularly spaced coconut trees, as in these cases the canopy cover overlaps will be minimal.

As an extended application of ITD, and solely for demonstration purposes, estimation of uniformity index, $PH^3$50, at plot-levels is presented as a part of this study. In our case, $PH^3$50 values ranged from 0.0432 to 0.451 (Table 6), revealing high irregularities – which imply notable variations in tree heights – in a number of plots. Since, there had been no previously published studies done in this direction, focusing on coconut plantations, our inference – that almost 80% (15 of 19 cases) of the total plots exhibit high heterogeneity – solely relies on the findings reported by authors who conducted similar studies in other major plantation crops of Brazil (Hentz et al., 2018; Hakamada et al., 2015a; Zucon et al., 2015; Hakamada et al., 2015b); exhaustive research targeted at coconut plantations would be able to append more clarity and applicability to the presented approach. For instance, Hakamada et al. (2015a) performed extensive study on clonal *Eucalyptus* forests for investigating the behavior of the uniformity between trees along a rotation and its relationship with the productivity and arrived at a conclusion highlighting the importance of homogenous supply of resources within plots and suggested that for stands to be considered uniform, Pv50 (for volume in this case) value should be in the range of 37–50%. Campoe (2012) obtained comparable results in *Eucalyptus grandis* stands, where the 20% larger trees of the stands were noted to acquire higher light efficiency in relation to the 20% smaller ones. As calculation of heights deemed more justifiable in case of younger plants, another study, undertook by Hentz et al. (2018) evaluated the forest uniformity in terms of $PH^3$50 index. Here, the authors compared the performance of two different UAV-based tree height calculation approaches in estimating $PH^3$50 index - of *Eucalyptus* spp. and *Pinus taeda* L plantations –with respect to field data and found the study sites to have $PH^3$50 index values greater than 0.34 and classified them as homogenous stands. Another interesting inference made was that the errors aggregating from tree height calculation does not influence the uniformity index results significantly as these errors are generally distributed evenly among the individual trees; even then, uniform index error reduction up to 2.79% was found attainable with careful selection of height calculation methods. Along the same line, Zucon et al. (2015) also observed that the influence of issues associated with UAV-based crown delineations had very nominal impact on accuracy of Pvar50 values in a young Eucalyptus plantation.

In case of coconut plantations, it is often the case that due to tree mortality in the initial phases, a lot of additional saplings are planted at a later stage, resulting in increased stand heterogeneity. Differences in silvicultural practices such as soil preparation, weed control, fertilizer treatment and number of trees per hectare also add to the overall heterogeneity (Ryan et al., 2010; Stape et al., 2010; Little et al., 2003; Silva, 2005; Örlander et al., 2002; Nilsson and Allen, 2003). Understanding these variations in the early stages are crucial for optimizing production as the responses of fertilization and several silvicultural practices are more pronounced at this growth period (Borders et al., 2004; Martinez-Vilalta et al., 2007). For instance, in case of plot 14, where the corresponding uniformity index was 0.0432, it can be noticed that the mean tree height was only 0.30 m. Therefore, proper application of fertilization and management practices has the potential to enhance homogeneity in these types of stands. Whereas, with plot 5, the standard deviation was very striking. This was due to the influence of a single tree – that was almost three times as tall as the remaining trees – and it greatly affected the uniformity index. Despite that, when we calculated the same, without considering the aforementioned tree, the uniformity index increased from an initial 0.1432 to 0.4036, which emphasizes the necessity for careful consideration of outliers for drawing meaningful interpretations. With regard to ITD, in general, stands with higher uniformity is expected to enhance tree detection accuracy, as in case of heterogenous stands, the taller trees with larger crown shapes might increase the amount of overlaps or even cause occlusion (Hyyppä et al., 2008; Silva et al., 2016). However, based on our results, which does not reveal any significant pattern in the aforementioned angle, we recommend future studies to take into consideration heights of individual trees and perform comparison studies for unfolding the intricacies; extraction of fruitful information on influence of forest uniformity and ITD is very limited from plot-level assessments. Also, since, uniformity index can be derived only after performing ITD, studies on the influence of this entity on ITD is wholly for advancing scientific perspectives and this index cannot be considered as a stand-alone determinant, such as COV, for enhancing ITD accuracy. In spite of that, we advocate research endeavors for evaluating combinations of pixel size and ITD methods for ITD and impact of forest uniformity assessment in mere future.

To reiterate, for successful identification of tree locations, in-depth understanding of TWS and SWS determination, with respect to COV, is vital as proved from our observations and similar studies (Silva et al., 2016; Wulder et al., 2000). With the emerging growth of software technology, algorithm development and remote sensing platforms, applications, and functionalities of ITD are expected to expand, and thereby assist the forest sector extensively; herein, we presented plot-level uniformity index estimation as an extension of ITD. Research focused on ITD in areas with multiple species types will be highly intriguing in this regard. The results from our study underscores that successful selection of TWS and SWS depending on tree crown structure, within-plot tree distribution patterns and canopy cover is crucial for developing adaptive ITD models based on LM algorithm. However, species-specific issues need to be carefully considered, and further research on forest uniformity and tree spacing's influence is also required to corroborate the applicability of the proposed methodology. Application of the template matching algorithm, provided by advance software like eCognition, or state-of-the-art visual analytic and multi-spectral lidar based techniques, might offer more clarity in this regard

(Huo et al., 2018; Olofsson et al., 2006; Gavazzi et al., 2016; Murugesan et al., 2017; Zhao et al., 2018); nonetheless, the cost of attaining these software license and high quality data can be a hurdle for small-scale users. To address issues regarding omission errors faced by certain TWS-SWS combinations, like in our case (7 × 7-5 × 5 TWS-SWS combination results for Type A Stands), additional studies, involving a wide range of complementing tree level variables - such as crown diameter, stem volume, tree basal area, etc. - are advocated. Also, we recommend evaluating the role of external factors such as climate, season, wind, etc. as well as impact of dried or diseased coconut leaves, which might affect the quality and output of the ITD workflow; this was beyond the scope of this paper. In addition, development in UAV technology has made it possible to have multiple cameras attached to UAV quadcopters, and that way take images in different wavelengths – of the same locations at the same instant - and hence, we expect to find a considerable amount of applications integrating features of UAV lidar data with optical as well as hyperspectral imagery in the mere future (Zhao et al., 2018; Yao and Wei, 2013; Caughlin et al., 2016; Sankey et al., 2017; Kandare et al., 2017). In sum, through our research we extended the usage of ITD phenomenon to trees with irregular and attenuated canopy covers such as coconut trees, and provided recommendations for assisting plantation owners, investors, and companies that rely on coconut production. Even though our study focused on a plantation in Brazil, we expect our work to conceivably pave the way for further research advancements in ITD and coconut plantation management spheres of a wider spectrum.

5. Conclusions

Lidar data along with suitable tree detection algorithm and window sizes – based on lidar-derived canopy cover - can be effectively used for delineating individual trees and thereby estimating a wide range of tree and canopy characteristics. This study was performed to detect individual coconut trees from a plantation having plots of varying canopy cover levels and presents an extended application of ITD, which is estimation of plot-level uniformity index. By employing a LM algorithm, we tested various combinations of TWS and SWS for achieving optimal ITD rates. Our results emphasize the importance of TWS and SWS parameter selection, depending on species types, forest structure and management objectives, and demonstrates the potential of ITD algorithm in attaining satisfactory results in cases of trees with irregular and attenuated canopy structures such as coconut trees. Future research focusing on integrating UAV-derived images, hyperspectral imagery, and satellite images with lidar data can further assist the efficient detection of individual trees in coconut plantations as well as forest areas having multiple species types.

Author contributions

Conceptualization, methodology, software, validation: M.M., B.A.F.M. C.A.S. and C.K.; formal analysis, investigation, resources: B.A.F.M., E.J.G.A. and M.A.M.; data curation, visualization, supervision, writing-review & editing: M.M., B.A.F.M., C.A.S., A.S.S.R. and A.C.

Funding

This research received no external funding

Declaration of Competing Interest

The authors declare no conflict of interest.

Acknowledgments

The authors would like to thank professors of Department of Forestry and Environmental Resources at North Carolina State University for offering the required pre-training for analyzing lidar data; Jason Rolfe, Paul Velte, and the JH Natural Resource Consultants, for their support and efforts regarding this study's initial phase, which was with UAVs; Mirza Asif, Wan-Shafrina Wan-Mohd-Jaafar, Gopika Gopan, Pransai Cheewakumnuan, Gonesh Chandra Saha, Prahlad Jat, Ken Junyawat, Beena Maheswari, Andre White, free3d.com and CGTrader community for the 3D modeling and research support; Swetha Narasimhan for her support with manuscript editing; Instituto de Terras e Cartografia do Estado do Rio de Janeiro – ITERJ for providing the lidar data that made this study happen. Also, the authors sincerely thank and are grateful to a group of anonymous reviewers for their valuable suggestions and recommendations that helped improve the manuscript significantly.

Appendix A. Supplementary data

Supplementary material related to this article can be found, in the online version, at doi:https://doi.org/10.1016/j.ecolmodel.2019.108736.

References

Alvares, C.A., Stape, J.L., Sentelhas, P.C., Gonçalves, J.L.M., Sparovek, G., 2013. Köppen's climate classification map for Brazil. Meteorol. Z. 22 (6), 711–728.
Andersen, H.E., 2009. Using airborne light detection and ranging (LIDAR) to characterize forest stand condition on the Kenai Peninsula of Alaska. West. J. Appl. For. 24 (2), 95–102.
Asner, G.P., Heidebrecht, K.B., 2002. Spectral unmixing of vegetation, soil and dry carbon cover in arid regions: comparing multispectral and hyperspectral observations. Int. J. Remote Sens. 23 (19), 3939–3958.
Bagaram, M., Giuliarelli, D., Chirici, G., Giannetti, F., Barbati, A., 2018. UAV remote sensing for biodiversity monitoring: are forest canopy gaps good covariates? Remote Sens. 10 (9), 1397.
Bai, Y., Walsworth, N., Roddan, B., Hill, D.A., Broersma, K., Thompson, D., 2005. Quantifying tree cover in the forest–grassland ecotone of British Columbia using crown delineation and pattern detection. For. Ecol. Manage. 212 (1-3), 92–100.
Binkley, D., 2004. A hypothesis about the interaction of tree dominance and stand production through stand development. For. Ecol. Manage. 190 (2-3), 265–271.
Binkley, D., Stape, J.L., Bauerle, W.L., Ryan, M.G., 2010. Explaining growth of individual trees: light interception and efficiency of light use by Eucalyptus at four sites in Brazil. For. Ecol. Manage. 259 (9), 1704–1713.
Binkley, D., Stape, J.L., Ryan, M.G., Barnard, H.R., Fownes, J., 2002. Age-related decline in forest ecosystem growth: an individual-tree, stand-structure hypothesis. Ecosystems 5 (1), 58–67.
Borders, B.E., Will, R.E., Markewitz, D., Clark, A., Hendrick, R., Teskey, R.O., Zhang, Y., 2004. Effect of complete competition control and annual fertilization on stem growth and canopy relations for a chronosequence of loblolly pine plantations in the lower coastal plain of Georgia. For. Ecol. Manage. 192 (1), 21–37.
Boyden, S., Binkley, D., Stape, J.L., 2008. Competition among Eucalyptus trees depends on genetic variation and resource supply. Ecology 89 (10), 2850–2859.
Campoe, O.C., 2012. Ecologia da produção e da competição intra-específica do Eucalyptus grandis ao longo de um gradiente de produtividade no estado de São Paulo. Doctoral dissertation. Universidade de São Paulo.
Cardil, A., Vepakomma, U., Brotons, L., 2017. Assessing pine processionary moth defoliation using unmanned aerial systems. Forests 8 (10), 402.
Cardil, A., Otsu, K., Pla, M., Silva, C.A., Brotons, L., 2019. Quantifying pine processionary moth defoliation in a pine-oak mixed forest using unmanned aerial systems and multispectral imagery. PlosOne 14 (3), e0213027.
Carvalho, R.R., Souza, P.E., Warwick, D., Pozza, E.A., Carvalho Filho, J.L.D., 2013. Spatial and temporal analysis of stem bleeding disease in coconut palm in the state of sergipe, Brazil. Anais da Academia Brasileira de Ciências 85 (4), 1567–1576.
Caughlin, T.T., Rifai, S.W., Graves, S.J., Asner, G.P., Bohlman, S.A., 2016. Integrating Lidar-derived tree height and Landsat satellite reflectance to estimate forest regrowth in a tropical agricultural landscape. Remote Sens. Ecol. Conserv. 2 (4), 190–203.
Choudhury, D., 2002. Problems and prospects of coconut cultivation in Assam. Indian Coconut J. 32 (10), 10–12.
Climate-data.org, 2014. Climograma Japeri. Accessed 18 Aug 2018. http://climate-data.org/.
de Azevedo, P.V., de Sousa, I.F., da Silva, B.B., da Silva, V.D.P.R., 2006. Water-use efficiency of dwarf-green coconut (Cocos nucifera L.) orchards in northeast Brazil. Agric. Water Manag. 84 (3), 259–264.
Dempewolf, J., Nagol, J., Hein, S., Thiel, C., Zimmermann, R., 2017. Measurement of within-season tree height growth in a mixed forest stand using UAV imagery. Forests 8 (7), 231.
Duncanson, L., Dubayah, R., 2018. Monitoring individual tree-based change with airborne lidar. Ecol. Evol. 8 (10), 5079–5089.
Edson, C., Wing, M.G., 2011. Airborne light detection and ranging (Lidar) for individual tree stem location, height, and biomass measurements. Remote Sens. 3 (11),

2494–2528.
Falkowski, M.J., Smith, A.M., Gessler, P.E., Hudak, A.T., Vierling, L.A., Evans, J.S., 2008. The influence of conifer forest canopy cover on the accuracy of two individual tree measurement algorithms using lidar data. Can. J. Remote. Sens. 34 (sup2), S338–S350.
Féret, J.B., Asner, G.P., 2013. Tree species discrimination in tropical forests using airborne imaging spectroscopy. IEEE Trans. Geosci. Remote. Sens. 51 (1), 73–84.
Ferraz, A., Mallet, C., Jacquemoud, S., Gonçalves, G.R., Tomé, M., Soares, P., et al., 2015. Canopy density model: a new ALS-derived product to generate multilayer crown cover maps. IEEE Trans. Geosci. Remote. Sens. 53 (12), 6776–6790.
Ferraz, A., Saatchi, S., Mallet, C., Meyer, V., 2016. Lidar detection of individual tree size in tropical forests. Remote Sens. Environ. 183, 318–333.
Gavazzi, G.M., Madricardo, F., Janowski, L., Kruss, A., Blondel, P., Sigovini, M., Foglini, F., 2016. Evaluation of seabed mapping methods for fine-scale classification of extremely shallow benthic habitats–application to the Venice Lagoon, Italy. Estuar. Coast. Shelf Sci. 170, 45–60.
Gebreslasie, M.T., Ahmed, F.B., Van Aardt, J.A., Blakeway, F., 2011. Individual tree detection based on variable and fixed window size local maxima filtering applied to IKONOS imagery for even-aged Eucalyptus plantation forests. Int. J. Remote Sens. 32 (15), 4141–4154.
Gibbs, H.K., Brown, S., Niles, J.O., Foley, J.A., 2007. Monitoring and estimating tropical forest carbon stocks: making REDD a reality. Environ. Res. Lett. 2 (4), 045023.
Gougeon, F.A., Moore, T., 1988. Individual tree classification using MEIS-II imagery. September. Geoscience and Remote Sensing Symposium, 1988. IGARSS'88. *Remote Sensing*: Moving Toward the 21st Century., International 2, 927.
Goutte, C., Gaussier, E., 2005. A probabilistic interpretation of precision, recall and F-score, with implication for evaluation. March. European Conference on Information Retrieval 345–359.
Hakamada, R.E., 2012. Uso do inventário florestal como ferramenta de monitoramento da qualidade silvicultura em povoamentos clonais de Eucalyptus. Doctoral dissertation. Universidade de São Paulo.
Hakamada, R.E., Stape, J.L., Camargo Zani de Lemos, C., Amaral Almeida, A.E., Silva, L.F., 2015a. Uniformidade entre árvores durante uma rotação e sua relação com a produtividade em Eucalyptus clonais. Cerne 21 (3).
Hakamada, R.E., Stape, J.L., Lemos, C.C.Z., Almeida, A.E.A., Silva, L.F., 2015b. Uso do inventário florestal e da uniformidade entre árvores como ferramenta de monitoramento da qualidade silvicultural em plantios clonais de eucalipto. Sci. For. 43 (105), 27–39.
Hall, F.G., Bergen, K., Blair, J.B., Dubayah, R., Houghton, R., Hurtt, G., et al., 2011. Characterizing 3D vegetation structure from space: mission requirements. Remote Sens. Environ. 115 (11), 2753–2775.
Harding, D.J., Lefsky, M.A., Parker, G.G., Blair, J.B., 2001. Laser altimeter canopy height profiles: methods and validation for closed-canopy, broadleaf forests. Remote Sens. Environ. 76 (3), 283–297.
Hentz, Â.M.K., Silva, C.A., Dalla Corte, A.P., Netto, S.P., Strager, M.P., Klauberg, C., 2018. Estimating forest uniformity in Eucalyptus spp. and Pinus taeda L. stands using field measurements and structure from motion point clouds generated from unmanned aerial vehicle (UAV) data collection. For. Syst. 27 (2), 005.
Hodgson, M.E., Bresnahan, P., 2004. Accuracy of airborne LiDAR-derived elevation. Photogramm. Eng. Remote Sensing 70 (3), 331–339.
Huo, L.Z., Silva, C.A., Klauberg, C., Mohan, M., Zhao, L.J., Tang, P., Hudak, A.T., 2018. Supervised spatial classification of multispectral LiDAR data in urban areas. PLoS One 13 (10), e0206185.
Hyyppä, J., Hyyppä, H., Leckie, D., Gougeon, F., Yu, X., Maltamo, M., 2008. Review of methods of small-footprint airborne laser scanning for extracting forest inventory data in boreal forests. Int. J. Remote Sens. 29 (5), 1339–1366.
Isenburg, M., 2015. LAStools—Efficient Tools for Lidar Processing. Accessed October 3, 2015. < lastools.org > . .
Jaafar, W.S.W.M., Woodhouse, I.H., Silva, C.A., Omar, H., Maulad, K.N.A., Hudak, A.T., Mohan, M., 2018. Improving individual tree crown delineation and attributes estimation of tropical forest using airborne LiDAR data. Forests (under review).
Jeronimo, S.M., Kane, V.R., Churchill, D.J., McGaughey, R.J., Franklin, J.F., 2018. Applying LiDAR individual tree detection to management of structurally diverse forest landscapes. J. For. 116 (4), 336–346.
Kahlon, C.S., Li, B., Board, J., Dia, M., Sharma, P., Jat, P., 2018. Cluster and principle component analysis of soybean grown at various row spacings, planting dates and plant populations. Open Agric. 3 (1), 110–121.
Kandare, K., Ørka, H.O., Dalponte, M., Næsset, E., Gobakken, T., 2017. Individual tree crown approach for predicting site index in boreal forests using airborne laser scanning and hyperspectral data. Int. J. Appl. Earth Obs. Geoinf. 60, 72–82.
Kattenborn, T., Sperlich, M., Bataua, K., Koch, B., 2014. Automatic single palm tree detection in plantation using UAV-based photogrammetric point clouds. Remote Sens. Spatial Inf. Sci. 3.
Ke, Y., Quackenbush, L.J., 2011. A review of methods for automatic individual tree-crown detection and delineation from passive remote sensing. Int. J. Remote Sens. 32 (17), 4725–4747.
Khosravipour, A., Skidmore, A.K., Isenburg, M., Wang, T., Hussin, Y.A., 2013. Development of an algorithm to generate a lidar pit-free canopy height model. October. Proceedings of the Silvilaser Conference, Beijing, China.
Khosravipour, A., Skidmore, A.K., Isenburg, M., Wang, T., Hussin, Y.A., 2014. Generating pit-free canopy height models from airborne Lidar. Photogramm. Eng. Remote Sensing 80 (9), 863–872.
Korpela, I., Anttila, P., Pitkänen, J., 2006. The performance of a local maxima method for detecting individual tree tops in aerial photographs. Int. J. Remote Sens. 27 (6), 1159–1175.
Koukoulas, S., Blackburn, G.A., 2005. Mapping individual tree location, height and species in broadleaved deciduous forest using airborne LIDAR and multi-spectral remotely sensed data. Int. J. Remote Sens. 26 (3), 431–455.
Kraus, K., Pfeifer, N., 1998. Determination of terrain models inwooded areas with airborne laser scanner data. Isprs J. Photogramm. Remote. Sens. 53, 193–203.
Kwak, D.A., Lee, W.K., Lee, J.H., Biging, G.S., Gong, P., 2007. Detection of individual trees and estimation of tree height using Lidar data. J. For. Res. 12 (6), 425–434.
Larsen, M., Eriksson, M., Descombes, X., Perrin, G., Brandtberg, T., Gougeon, F.A., 2011. Comparison of six individual tree crown detection algorithms evaluated under varying forest conditions. Int. J. Remote Sens. 32 (20), 5827–5852.
Leckie, D., Gougeon, F., Hill, D., Quinn, R., Armstrong, L., Shreenan, R., 2003. Combined high-density lidar and multispectral imagery for individual tree crown analysis. Can. J. Remote. Sens. 29 (5), 633–649.
Lelong, C., Lesponne, C., Lamanda, N., Lainé, G., Malézieux, E., 2004. Understanding the Spatial Structure of Agroforestry Systems Using Very High Resolution Remote Sensing: an Application to Coconut-based Systems in Melanesia.
Li, W., Guo, Q., Jakubowski, M.K., Kelly, M., 2012. A new method for segmenting individual trees from the lidar point cloud. Photogramm. Eng. Remote Sens. 78, 75–84.
Lindberg, E., Hollaus, M., 2012. Comparison of methods for estimation of stem volume, stem number and basal area from airborne laser scanning data in a hemi-boreal forest. Remote Sens. 4 (4), 1004–1023.
Little, K.M., Van Staden, J., Clarke, G.P.Y., 2003. Eucalyptus grandis x E. camaldulensis variability and intra-genotypic competition as a function of different vegetation management treatments. New For. 25 (3), 227–242.
Luu, T.C., Binkley, D., Stape, J.L., 2013. Neighborhood uniformity increases growth of individual Eucalyptus trees. For. Ecol. Manage. 289, 90–97.
Martinez-Vilalta, J., Vanderklein, D., Mencuccini, M., 2007. Tree height and age-related decline in growth in Scots pine (Pinus sylvestris L.). Oecologia 150 (4), 529–544.
Martins, C.R., Jesus Junior, L.A., 2011. Evolução da produção de coco no Brasil e o comércio internacional: panorama 2010. Aracaju: Embrapa Tabuleiros Costeiros. 28 p. (Embrapa Tabuleiros Costeiros. Documentos, 164), Accessed 18 Aug. 2018. Ministério do Desenvolvimento, Indústria e Comércio; Secretaria de Comércio Exterior. Aliceweb, BRASIL. http://www.cpatc.embrapa.br/publicacoes_2011/doc_164.pdf.
Martins, C.R., Jesus Junior, L.A., 2014. Produção e comercializaçõao de coco no Brasil frente ao comércio internacional : panorama 2014. Aracaju: Embrapa Tabuleiros Costeiros. 51 p. (Embrapa Tabuleiros Costeiros. Documentos, 164), Accessed 18 Aug. 2018. Ministério do Desenvolvimento, Indústria e Comércio; Secretaria de Comércio Exterior. Aliceweb, BRASIL. https://ainfo.cnptia.embrapa.br/digital/bitstream/item/122994/1/Producao-e-comercializacao-Doc-184.pdf.
Mayossa, P.C.K., D'eeckenbrugge, G.C., Borne, F., Gadal, S., Viennois, G., 2015. Developing a method to map coconut agrosystems from high-resolution satellite images. August. 27th International Cartographic Conference 16th General Assembly.
McGauchey, R.J., 2015. FUSION/LDV: Software for Lidar Data Analysis and Visualization. Accessed Oct. 15 2015. Forest Service Pacific Northwest Research Station USDA, Seattle. http://forsys.cfr.washington.edu/fusion/FUSIONmanual.pdf.
Mohan, M., Silva, C.A., Klauberg, C., Jat, P., Catts, G., Cardil, A., et al., 2017. Individual tree detection from unmanned aerial vehicle (UAV) derived canopy height model in an open canopy mixed conifer forest. Forests 8 (9), 340.
Monnet, J.M., Mermin, E., Chanussot, J., Berger, F., 2010. Tree top detection using local maxima filtering: a parameter sensitivity analysis. 10th International Conference on LiDAR Applications for Assessing Forest Ecosystems (Silvilaser 2010). September, (pp. 9-p).
Murugesan, S., Bouchard, K., Chang, E., Dougherty, M., Hamann, B., Weber, G.H., 2017. Multi-scale visual analysis of time-varying electrocorticography data via clustering of brain regions. BMC Bioinformatics 18 (6), 236.
Nilsson, U., Allen, H.L., 2003. Short-and long-term effects of site preparation, fertilization and vegetation control on growth and stand development of planted loblolly pine. For. Ecol. Manage. 175 (1-3), 367–377.
Nunes, M.H., Ewers, R.M., Turner, E.C., Coomes, D.A., 2017. Mapping aboveground carbon in oil palm plantations using LiDAR: a comparison of tree-centric versus area-based approaches. Remote Sens. 9 (8), 816.
Nyamgeroh, B.B., Groen, T.A., Weir, M.J., Dimov, P., Zlatanov, T., 2018. Detection of forest canopy gaps from very high resolution aerial images. Ecol. Indic. 95, 629–636.
Ohler, J.G., 1998. Back matter-modern coconut management. Modern Coconut Management: Palm Cultivation and Products. Practical Action Publishing, pp. 409–458.
Olofsson, K., Wallerman, J., Holmgren, J., Olsson, H., 2006. Tree species discrimination using Z/I DMC imagery and template matching of single trees. Scand. J. For. Res. 21 (S7), 106–110.
Örlander, G., Nordborg, F., Gemmel, P., 2002. Effects of Complete Deep-Soil Cultivation on Initial Forest Stand Development (No. 213).
Otto, M.S.G., Hubbard, R.M., Binkley, D., Stape, J.L., 2014. Dominant clonal Eucalyptus grandis× urophylla trees use water more efficiently. For. Ecol. Manage. 328, 117–121.
Persson, A., Holmgren, J., Soderman, U., 2002. Detecting and measuring individual trees using an airborne laser scanner. Photogramm. Eng. Remote Sensing 68 (9), 925–932.
Pinz, A.J., 1991. A Computer Vision System for the Recognition of Trees in Aerial Photographs.
Pont, D., Kimberley, M.O., Brownlie, R.K., Sabatia, C.O., Watt, M.S., 2015. Calibrated tree counting on remotely sensed images of planted forests. Int. J. Remote Sens. 36 (15), 3819–3836.
Puttemans, S., Van Beeck, K., Goedemé, T., 2018. Comparing boosted cascades to deep learning architectures for fast and robust coconut tree detection in aerial images. January. Proceedings of the International Conference on Computer Vision Theory and Applications.
R Core Team, 2015. R: A Language and Environment for Statistical Computing. R

Foundation for Statistical Computing, Vienna, Austria. Available online: http://www.R-project.org (Accessed on 15 October 2015).
Roise, J.P., Harnish, K., Mohan, M., Scolforo, H., Chung, J., Kanieski, B., et al., 2016. Valuation and production possibilities on a working forest using multi-objective programming, Woodstock, timber NPV, and carbon storage and sequestration. Scand. J. For. Res. 31 (7), 674–680.
Roussel, J.R., Auty, D., 2018. lidR: Airborne LiDAR Data Manipulation and Visualization for Forestry Applications. R package. Available online: https://github.com/Jean-Romain/lidR (Accessed on 31 January 2018). .
Ryan, M.G., Stape, J.L., Binkley, D., Fonseca, S., Loos, R.A., Takahashi, E.N., et al., 2010. Factors controlling Eucalyptus productivity: how water availability and stand structure alter production and carbon allocation. For. Ecol. Manage. 259 (9), 1695–1703.
Saha, G.C., Mat, R.C., 2018a. A study of coconut plantation management practice: problems and Status. SMMTC Postgraduate Symposium 2018. March, (p. 220).
Saha, G.C., Mat, R.C., 2018b. 3D visualization of GIS data in coconut plantation management: challenges and opportunities. IOP Conference Series: Earth and Environmental Science June, (Vol. 169, No. 1, p. 012068).
Samarajeewa, S., Ratnasiri, N.G.S.C., Thanaweeraarachchi, P.T., 2001. Supply Response of Coconut Production in Sri Lanka.
Sankey, T., Donager, J., McVay, J., Sankey, J.B., 2017. UAV lidar and hyperspectral fusion for forest monitoring in the southwestern USA. Remote Sens. Environ. 195, 30–43.
Satyanand, P.N., 2009. Developing Countries Now Dominate Global Agricultural Plantation Business. September, Retrieved from. http://www.thehindu.com.
Schneider, E.E., Larson, A.J., 2017. Spatial aspects of structural complexity in Sitka spruce–western hemlock forests, including evaluation of a new canopy gap delineation method. Can. J. For. Res. 47 (8), 1033–1044.
Schreuder, H.T., Gregoire, T.G., Wood, G.B., 1993. Sampling Methods for Multiresource Forest Inventory. John Wiley & Sons.
Silva, C.A., Crookston, N.L., Hudak, A.T., Vierling, L.A., Klauberg, C., Silva, M.C.A., 2017a. Package 'rLiDAR'.
Silva, C.A., Hudak, A.T., Vierling, L.A., Loudermilk, E.L., O'Brien, J.J., Hiers, J.K., et al., 2016. Imputation of individual Longleaf Pine (Pinus palustris Mill.) Tree attributes from field and Lidar data. Can. J. Remote. Sens. 42 (5), 554–573.
Silva, C.A., Klauberg, C., Hudak, A.T., Vierling, L.A., Jaafar, W.S.W.M., Mohan, M., et al., 2017b. Predicting stem total and assortment volumes in an industrial Pinus taeda L. Forest plantation using airborne laser scanning data and random forest. Forests 8 (7), 254.
Silva, C.A., Valbuena, R., Pinagé, E.R., Mohan, M., de Almeida, D.R.A., Broadbent, E.N., et al., 2019. ForestGapR: an r package for forest gap analysis from canopy height models. Methods Ecol. Evol.
Silva, C.R.D., 2005. Efeito do espaçamento e arranjo de plantio na produtividade e uniformidade de clones de Eucalyptus na região nordeste do Estado de São Paulo. Doctoral dissertation. Universidade de São Paulo.
Sokolova, M., Japkowicz, N., Szpakowicz, S., 2006. Beyond accuracy, F-score and ROC: a family of discriminant measures for performance evaluation. December. Australasian Joint Conference on Artificial Intelligence 1015–1021.
Srestasathiern, P., Rakwatin, P., 2014. Oil palm tree detection with high resolution multi-spectral satellite imagery. Remote Sens. 6 (10), 9749–9774.
Srinivasan, N., 2002. Coconut leaf rot complex and perspectives for the disease control. Indian Coconut J. 32 (9), 2.
Stape, J.L., Binkley, D., Ryan, M.G., Fonseca, S., Loos, R.A., Takahashi, E.N., et al., 2010. The Brazil Eucalyptus Potential Productivity Project: influence of water, nutrients and stand uniformity on wood production. For. Ecol. Manage. 259 (9), 1684–1694.
Teina, R., 2009. Caractérisation de la cocoteraie des Tuamotu à partir d'images satellites à très haute résolution spatiale. Doctoral dissertation. Université Pierre et Marie Curie-Paris VI.
White, J.C., Tompalski, P., Coops, N.C., Wulder, M.A., 2018. Comparison of airborne laser scanning and digital stereo imagery for characterizing forest canopy gaps in coastal temperate rainforests. Remote Sens. Environ. 208, 1–14.
Wulder, M.A., Dechka, J.A., Gillis, M.A., Luther, J.E., Hall, R.J., Beaudoin, A., Franklin, S.E., 2003. Operational mapping of the land cover of the forested area of Canada with Landsat data: EOSD land cover program. For. Chron. 79 (6), 1075–1083.
Wulder, M.A., White, J.C., Nelson, R.F., Næsset, E., Ørka, H.O., Coops, N.C., et al., 2012. Lidar sampling for large-area forest characterization: a review. Remote Sens. Environ. 121, 196–209.
Wulder, M., Niemann, K.O., Goodenough, D.G., 2000. Local maximum filtering for the extraction of tree locations and basal area from high spatial resolution imagery. Remote Sens. Environ. 73 (1), 103–114.
Xiao, C., Qin, R., Huang, X., 2018. Individual tree detection from multi-view satellite images. IGRASS 2018.
Yao, W., Wei, Y., 2013. Detection of 3-D individual trees in urban areas by combining airborne Lidar data and imagery. IEEE Geosci. Remote. Sens. Lett. 10 (6), 1355–1359.
Zhang, W., Ke, Y., Quackenbush, L.J., Zhang, L., 2010. Using error-in-variable regression to predict tree diameter and crown width from remotely sensed imagery. Can. J. For. Res. 40 (6), 1095–1108.
Zhao, X., Wu, Y., Lee, D.L., Cui, W., 2018. iForest: interpreting random forests via visual analytics. IEEE Transactions on Visualization and Computer Graphics.
Zhen, Z., Quackenbush, L.J., Zhang, L., 2016. Trends in automatic individual tree crown detection and delineation—evolution of lidar data. Remote Sens. 8 (4), 333.
Zucon, A.R.S., Hawkes, B., de Lemos, C.C.Z., Batistuzzo, G.Z.B., Hakamada, R.E., de Pontes, G.R., et al., 2015. Use of unmanned aerial vehicle images as a tool to evaluate stand uniformity in clonal Eucalyptus plantations. Anais do XVII Simpósio Bras Sensoriamento Remoto-SBSR, João Pessoa INPE. pp. 6381–6388.